

Kinetic and Solid State Degradation of Chitosan-Methacrylic acid-N,N- methylenebisacrylamide (Cs-MAA-MBA) Dual-responsive Hydrogels

Muhammad Bisyrul Hafi Othman¹, Hazizan Md Akil^{1*}, Abbas Khan², Zulkifli Ahmad¹, and
Siti Zalifah Md Rasib¹

¹School of Materials and Mineral Resources Engineering, Engineering Campus, Universiti Sains Malaysia, Seri
Ampangan, 14300 Nibong Tebal Pulau Pinang

²Department of Chemistry, Abdul Wali Khan University Mardan, 23200 Pakistan

ABSTRACT: Chitosan-based dual responsive hydrogels, at different compositions of methacrylic acid (MAA) and N,N-methylenebisacrylamide (MBA), were synthesised by free radical copolymerization method in water. The non-isothermal degradation behaviour of synthesized hydrogels was studied by ThermoGravimetric Analysis (TGA) under nitrogen purge. In this study, the kinetic degradation parameters were clarified using the Kissinger method and the solid state degradation mechanism was evaluated using the Coats-Redfern (C-Red) method. It is clearly observed that the E_a curve, computed using Kissinger methods, has a similar change trend with the Flynn-Wall-Ozawa (F-W-O) method. However, $E_{a\text{F-W-O}} > E_{a\text{Kissinger}}$ about 0.2 to 10.67 kJmol⁻¹, because the β in $\ln \beta/T$ Kissinger method depends on the function of temperature compared to $\log \beta$ in the F-W-O method. Three types of solid state processes at β of 20 °Cmin⁻¹ in nitrogen atmosphere were proposed as F1, F2 and F3, depending on the optimum composition of MAA. To adapt to this contrast, we propose that the decomposition of Cs-MAA-MBA hydrogels series could be governed mainly by the molecular structure and kinetic consideration, and that the solid state degradation process is dependent on the composition.

KEYWORDS: Chitosan (Cs); Thermal stability; Kinetic; Activation energy (E_a); Solid state; Methacrylic acid (MAA)

Nomenclatures (SI unit)/ Abbreviations

COO ⁻	Carboxylate ion
NH ₃ ⁺	Ammonium ion
3D	Three-dimensional
α	Conversion
β	Heating rate; (Kmin ⁻¹)
d α /dt	Rate of conversion
d ² α /dt ²	Rate of conversion for second derivative thermogravimetry
$f(\alpha)$	Expression of kinetic model
A	Pre-exponential factor (min ⁻¹)
APS	Ammonium persulphate
ASTM	American Society for Testing and Materials
Cs	Chitosan

International Journal of Innovative Research in Science, Engineering and Technology

(An ISO 3297: 2007 Certified Organization)

Vol. 5, Special Issue 12, May 2016

Cs-MAA	Chitosan-Methacrylic acid chain
Cs-MAA-MAA	Chitosan-Methacrylic acid-Methacrylic acid chain
Cs-MAA-MBA	Chitosan-Methacrylic acid-N,N-methylenebisacrylamide chain
Cs-MBA	Chitosan-N,N-methylenebisacrylamide chain
Cs-Cs	Chitosan-Chitosan chain
c	Intercept-y
DDH ₂ O	Deionised distilled water
DDTG	Second derivative thermogravimetry
DSC	Differential scanning calorimetry
DTG	Derivative thermogravimetry
E_a	Activation energy (kJmol ⁻¹)
Eq	Equation
F-W-O	Flynn-Wall-Ozawa
$g(\alpha)$	Expression of kinetic model
k	Rate constant
M_o	Initial mass (g)
M_t	Mass at time (g)
M_f	Final mass (g)
MBA	N,N-methylenebisacrylamide
MAA	Methacrylic acid
MAA-MAA	Methacrylic acid-Methacrylic acid chain
MAA-MBA	Methacrylic acid-N,N-methylenebisacrylamide chain
MBA-MBA	N,N-methylenebisacrylamide-N,N-methylenebisacrylamide chain
M_w	Mass average molar mass (gmol ⁻¹)
n	Kinetic order
N ₂	Nitrogen gas
PMAA	Polymethylacrylate Acid
T_5	Temperature at 5% mass loss (K)
T_{10}	Temperature at 10% mass loss (K)
R	Gas constant (8.314 Jmol ⁻¹ K ⁻¹)
R_w	Residue mass (g)
T_d	Temperature at maximum mass loss (K)
TG	Thermogravimetry
T_g	Glass transition temperature
T	Temperature (K)
t	Time (min)

I.INTRODUCTION

Recently, many studies have sought to identify the desirable properties of Chitosan (Cs) microgel based for potential industrial applications; including the modification of Cs by chemical/physical methods and compounding with other moieties (Dimida et al., 2015; Mueh Julkapli et al., 2011; Rami et al., 2014). However, very little has been published on the effect of degradability related to gelation and chain-relaxation of its component compositions, on solid state thermal degradation mechanism and kinetics study. In previously published paper (Khan et al., 2013; Othman et al., 2015), the influence of MBA and MAA contents in Cs based hydrogels on kinetic degradation behaviour using the Flynn-Wall-Ozawa (F-W-O) method (Flynn, 1997; Ozawa, 1970) were reported. Kinetic parameters were calculated, and subsequently used to predict the influence of gel composition on lifetime, and evaluate the solid state degradation mechanism. The uniqueness of this work is that the physicochemical behaviour of these hydrogels is dependent on the hydrogel's composition.

Even though the mathematical description of the decomposition process of polymers relies on the three kinetic components of two Arrhenius parameters, which are apparent activation energy (E_a) and pre-exponential factor (A),

International Journal of Innovative Research in Science, Engineering and Technology

(An ISO 3297: 2007 Certified Organization)

Vol. 5, Special Issue 12, May 2016

they are also governed by the analytical expression describing the kinetic model $f(\alpha)$ and the decomposition process of polymers in a solid state. From previous experience, it is already known that kinetic analysis, based on single heating rate (β) methods (isothermal), is not dependable and encounters many problems. Therefore, in this paper, we intend to provide a partial explanation of multiple heating rate methods (non-isothermal), such as Kissinger(Kissinger, 1957), and the type of solid state mechanism using Coats-Redfern (C-Red)(Coats and Redfern, 1965).

By recognising the importance of understanding the kinetic thermal decomposition and solid state mechanism of Cs-based hydrogels, in this work, the apparent E_a was determined using the Kissinger and C-Red methods. The type of solid state mechanism was determined by C-Red method using F-W-O kinetic data at a low conversion, based on Doyle's approximation(Doyle, 1965). This study also aims to link previously studied isolated methods together, as well as to provide useful information on a wide range of related areas.

II.EXPERIMENTAL

2.1. Materials

N,N-methylenebisacrylamide (purity >95.0 %) and Chitosan ($M_w \approx 160,000$ g/mol, degree of deacetylation $\approx 91.0\%$) were purchased from Aldrich (St. Louis, MO, USA). All other chemicals were obtained from Acros (Geel, Belgium). Methacrylic acid (purity > 95.0%) was further purified through distillation under reduced pressure, whereas all other chemicals were used as received and without further purification. Deionised distilled water (ddH_2O), obtained from a Milli-Q® system, Millipore (Bedford, MA, USA), was used for all reactions, solution preparations, and microgel purifications.

2.2. Microgel synthesis

All microgel compositions were synthesised by free-radical copolymerisation of Cs, MAA and MBA, using Ammonium Per Sulphate (APS) as an initiator, following previously reported procedures (Khan et al., 2013). The composition, with codes of synthesized microgel samples, is summarised in **Table 1**.

Table 1
Summary of gel compositions

Cs-MAA- MBA Series	Composition of Gel (mg/100mL)		
	Cs	MAA	MBA
300:000:00 Cs pure	300	000	0
300:300:00	300	300	0
300:300:10	300	300	10
300:300:15	300	300	15
300:150:15	300	150	15
300:100:15	300	100	15

Cs-MAA- MBA Series FTIR spectrum (powder) $\nu_{max} = 3400$ to 3300 cm^{-1} (broad, O-H and N-H stretching), 2872 cm^{-1} (C-H stretching methyl groups of glycol Cs), 2872 cm^{-1} , 1373 cm^{-1} (C-H vibration), 1650 to 1560 cm^{-1} (carbonyl stretching of the amino group), 1253 , 1158 cm^{-1} (C-N stretching of the amino group of Cs, 1560 , 1150 , 894 cm^{-1} (saccharide structure of Cs), 1061.71 (broad, C-O stretching)(Khan et al., 2013).

Dynamic and non-isothermal TGA was carried out using a Perkin Elmer Pyris™ 6 TGA Thermogravimetry analyser according to E 1131 at $30-600$ °C with heating rates (β) of 5, 10, and 20 °C min^{-1} in N_2 atmosphere. Onset decomposition temperature (T_d), temperature at 5% mass loss (T_5), temperature at 10% mass loss (T_{10}), and residual mass (R_w) at 600 °C, were also determined. To measure the glass transition temperature (T_g), non-isothermal DSC was performed using a PerkinElmer DSC-6 Thermogravimetry analyser according to ASTM D 3418 at $40-200$ °C with a heating rate of 10 °C min^{-1} in N_2 . Finally, kinetic analysis via the Kissinger and C-Red methods was carried out at various β , i.e., 5, 10, and 20 °C min^{-1} . The type of solid state mechanism was determined by C-Red method using F-W-O kinetic data at a low conversion ($\alpha < 30$ %) based on Doyle's approximation.

International Journal of Innovative Research in Science, Engineering and Technology

(An ISO 3297: 2007 Certified Organization)

Vol. 5, Special Issue 12, May 2016

III.RESULTS AND DISCUSSION

3.1. Characteristics of the Microgels

The Cs-based microgels were prepared by the free-radical polymerisation of Cs, MAA, and MBA, using APS as an initiator with the proposed scheme based on previously reported work (Khan et al., 2013; Othman et al., 2015). The MAA and MBA contents were varied in the Cs-MAA-MBA compositions, to investigate the influence of content on thermal stability, degradation kinetic, and lifetime. Again, to promote diversity and maintain the physicochemical and thermo-responsive properties, the sequence of MAA/MBA or isomerism in the Cs-MAA-MBA hydrogels was not controlled in our study (Khan et al., 2013). In our previous study (Othman et al., 2015), the T_g of Cs-MAA-MBA samples was determined during the second heating process at around 130–160 °C with a β of 10 °Cmin⁻¹. In summary, the TG in a nitrogen atmosphere demonstrated a char yield that showed more than 30% residue for Cs and less than 25% residue for Cs derivatives, once the degradation was completed at 600 °C. The apparent E_a , determined using the F-W-O, found that the E_a was attributed to the greater cross-linking density of Cs hydrogel. Similarly, the lower swelling ability of Cs hydrogel may have been due to a slower relaxation rate of the polymer chain, which resulted in an increased lifetime of the potential drug-release rate.

Here, the apparent E_a will be determined using the Kissinger and C-Red methods. The data presented in this study will be extremely useful to fit the F-W-O method. Furthermore, the type of solid state mechanism was determined using the C-Red method that used the F-W-O kinetic data at low conversions based on Doyle's approximations.

3.2. Kinetic evaluation of Cs-MAA- MBA

In order to determine the kinetic parameters, such as reaction order (n), E_a , etc., thermogravimetric analysis (TGA) was applied. The rate of reaction was defined as the ratio of actual mass loss at time (t) to the total mass loss at complete degradation process (as shown in Eq. 1).

$$\alpha = \frac{M_o - M_t}{M_o - M_f} \quad (1)$$

where M_o , M_t , and M_f , are the initial mass of the sample, the mass of the sample at time, and the final mass, respectively, of the completely decomposed sample.

Generally, a typical kinetic process model for polymer degradation can be represented by the decomposition rate ($d\alpha/dt$); which is a function of the temperature and mass of the sample. It is assumed that the rates of conversion (α) are proportional to the concentration of the reacted material. Therefore, the rate of α can be expressed by the following basic rate equation (Eq. 2).

$$\frac{d\alpha}{dt} = k(T)f(\alpha) \quad (2)$$

where $d\alpha/dt$ is degradation rate, k is rate constant, $f(\alpha)$ is the differential expression of a kinetic model function (Table 2).

Table 2

Algebraic expressions for g(a) and f(a) for the most frequently used mechanisms of solid state processes

Mechanism	S	g(α)	f(α)
Nucleation and growth (Avrami Equation (1))	A2	$[-\ln(1-\alpha)]^{1/2}$	$2(1-\alpha)[- \ln(1-\alpha)]^{1/2}$
Nucleation and growth (Avrami Equation (2))	A3	$[-\ln(1-\alpha)]^{1/3}$	$3(1-\alpha)[- \ln(1-\alpha)]^{1/3}$
Nucleation and growth (Avrami Equation (3))	A4	$[-\ln(1-\alpha)]^{1/4}$	$4(1-\alpha)[- \ln(1-\alpha)]^{1/4}$
Phase boundary controlled reaction (one-dimensional movement)	R1	α	1

International Journal of Innovative Research in Science, Engineering and Technology

(An ISO 3297: 2007 Certified Organization)

Vol. 5, Special Issue 12, May 2016

Phase boundary controlled reaction (contracting area)	R2	$[1-(1-\alpha)]^{1/2}$	$2(1-\alpha)^{1/2}$
Phase boundary controlled reaction (contracting volume)	R3	$[1-(1-\alpha)]^{1/3}$	$3(1-\alpha)^{1/3}$
One-dimensional diffusion	D1	α^2	$(1/2)\alpha^{1-1}$
Two-dimensional diffusion (Valensi equation)	D2	$(1-\alpha)\ln(1-\alpha)+\alpha$	$-\ln(1-\alpha)^{-1}$
Three-dimensional diffusion (Jander equation)	D3	$[1-(1-\alpha)^{1/3}]^2$	$(3/2)[1-(1-\alpha)^{1/3}]^{-1}-(1-\alpha)^{2/3}$
Three-dimensional diffusion (Ginstling Brounshtein equation)	D4	$[1-(2/3)\alpha^{1/3}]-\alpha^{2/3}$	$(3/2)[1-(1-\alpha)^{1/3}]^{-1}$
Random nucleation with one nuclei on the individual particle	F1	$-\ln(1-\alpha)$	$1-\alpha$
Random nucleation with two nuclei on the individual particle	F2	$1/(1-\alpha)$	$(1-\alpha)^2$
Random nucleation with three nuclei on the individual particle	F3	$1/(1-\alpha)^2$	$(1-\alpha)^3$

Meanwhile, k is given by the Arrhenius Equation (Eq. 3) expression,

$$k = A \exp\left(-\frac{E_a}{RT}\right) \quad (3)$$

where A is the frequency factor (s^{-1}), E_a is the apparent kinetic energy of the degradation reaction (kJmol^{-1}), R is the gas constant, α and T is the absolute temperature. It can be assumed that k (from Eq. 1) follows the Arrhenius equation. Therefore, substituting Eq. 3 into Eq. 1 produces Eq. 4.

$$\frac{d\alpha}{dt} = A \exp\left(-\frac{E_a}{RT}\right) f(\alpha) \quad (4)$$

According to non-isothermal kinetic theory, thermal degradation data is generally performed by following Eq. 5 below.

$$\frac{d\alpha}{dt} = \beta \frac{d\alpha}{dT} = A \exp\left(-\frac{E_a}{RT}\right) f(\alpha) \quad (5)$$

where $\beta = dT/dt$ is a constant. By rearranging, Eq.5 can be simplified as Eq. 6 below.

$$\frac{d\alpha}{dt} = \frac{A}{\beta} \exp\left(-\frac{E_a}{RT}\right) f(\alpha) \quad (6)$$

where $f(\alpha)$ is the differential expression of a kinetic model function, β is the heating rate (K/min), E_a and A are, respectively, the E_a (kJ/mol) and the pre-exponential factor (min^{-1}) for the decomposition reaction. R is the gas constant ($8.314 \text{ Jmol}^{-1} \text{ K}^{-1}$).

Kissinger method (differential method)

The advantage of the Kissinger model is that E_a can be obtained without any advanced knowledge of thermal degradation reaction mechanism. The Kissinger method uses Eq. (7) to determine the E_a of solid state reactions.

International Journal of Innovative Research in Science, Engineering and Technology

(An ISO 3297: 2007 Certified Organization)

Vol. 5, Special Issue 12, May 2016

$$\ln\left(\frac{\beta}{T_p^2}\right) = \ln\frac{AR}{E_a} + \ln\left[n(1-\alpha_p)^{n-1}\right] - \frac{E_a}{RT} \quad (7)$$

where T_p and α_p are the absolute temperature and mass loss at maximum massloss rate $(da/dt)_p$, respectively, and n is the reaction order. From the slope of the straight line $\ln(\beta/T_p^2)$ versus $1/T_p$, the E_a can be obtained(as presented in Figure 1).

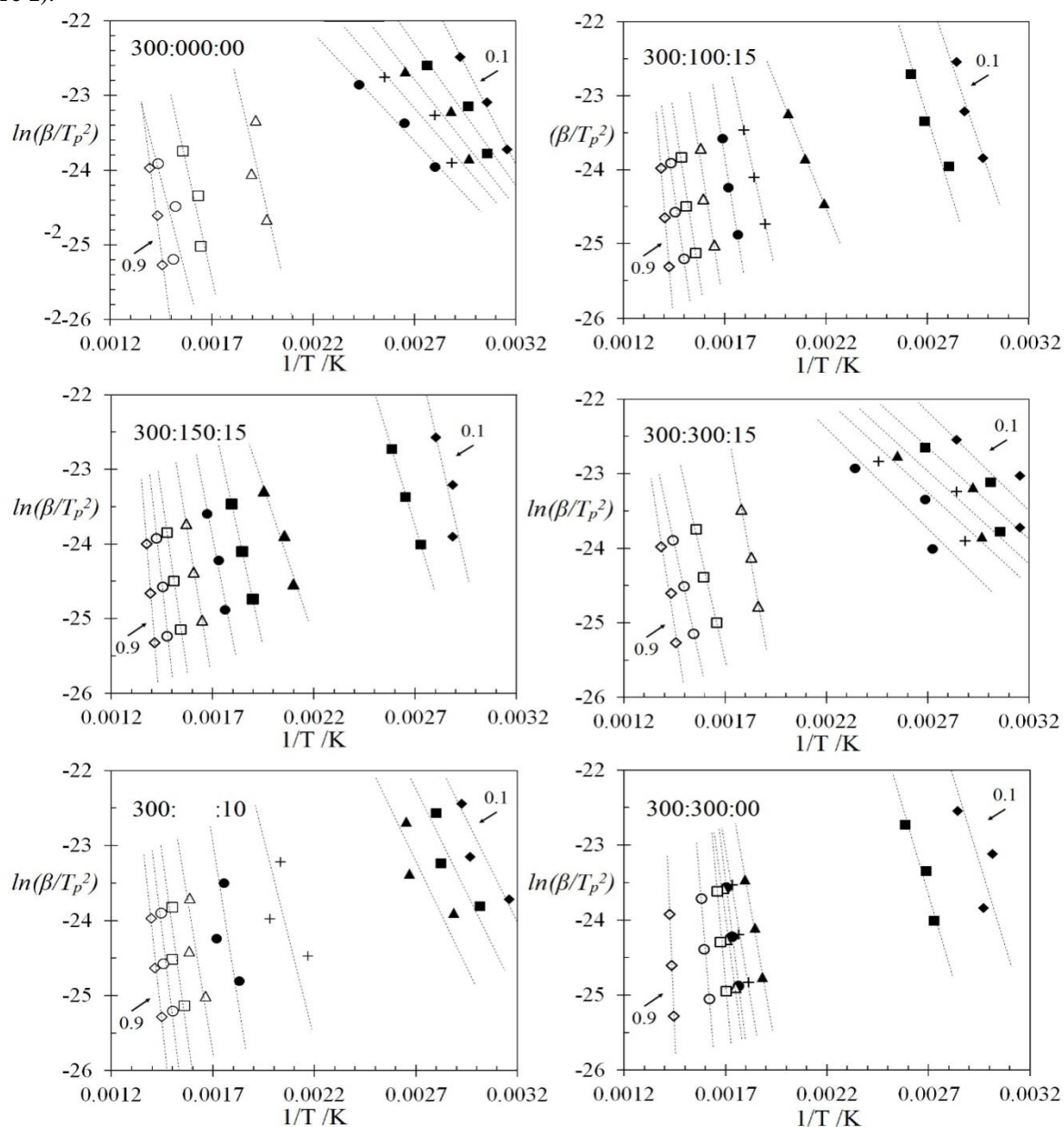


Fig. 1. Plot of $\ln(\beta/T_p^2)$ at different β according to the Kissinger method for the Cs-MAA-MBA series with mass loss from 10 % to 90% conversion ($\alpha \times 10^3$)

International Journal of Innovative Research in Science, Engineering and Technology

(An ISO 3297: 2007 Certified Organization)

Vol. 5, Special Issue 12, May 2016

From **Fig. 1**, the function of E_a versus α according to the Kissinger method of Cs-MAA-MBA series in nitrogen atmosphere at the different content of MAA and MBA can be plotted (**Fig. 2**). From previous literature (Barral et al., 1998; Criado and Ortega, 1986), the Kissinger method has been reported to provide highly reliable values of E_a with an error of less than 5%, independent of reaction mechanism, provided that $E_a/RT > 10$.

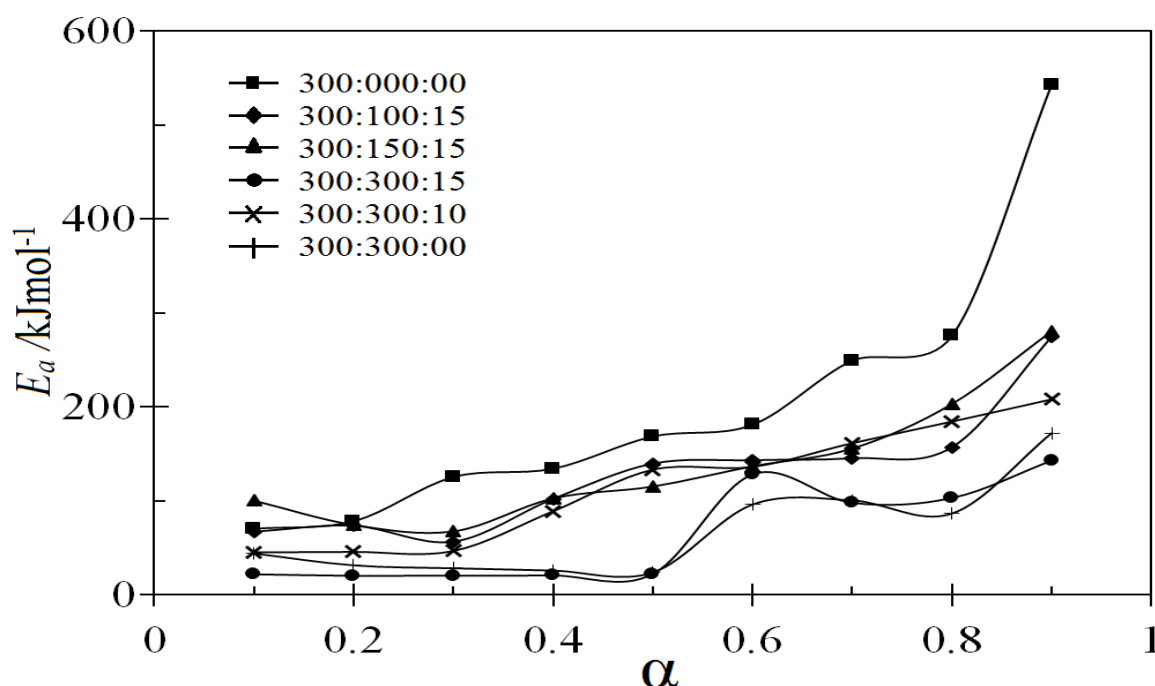


Fig. 2. Plot of E_a versus α according to the Kissinger method of the Cs-MAA-MBA series with mass loss from 10 % to 90% conversion in nitrogen.

The E_a values calculated (**Fig. 2**) were found to have an almost similar gradient and trends with that of the F-W-O method. Therefore, the results showed a negative value of E_a , which corresponds to the decrease in degradation rates in response to the increase in temperatures. By following an approximate exponential relationship between F-W-O and Kissinger methods, the rate constant can be fitted to the Arrhenius expression. **Table 3** shows the comparison of E_a versus α between F-W-O and Kissinger methods for the Cs-MAA-MBA series.

Table 3.

Comparison E_a versus α between F-W-O and Kissinger methods for the Cs-MAA-MBA series at $0.5 < \alpha$.

α	E_a (kJmol ⁻¹)		ΔE_a
	F-W-O	Kissinger	$E_{aF-W-O} - E_{aKissinger}$
300:000:00			
0.1	81.07	70.50	10.57
0.2	78.74	78.54	0.2
0.3	127.94	125.57	2.37
0.4	141.79	134.40	7.39
0.5	179.35	168.68	10.67
300:000:15			
0.1	86.70	77.41	9.29
0.2	64.27	73.72	-9.45

International Journal of Innovative Research in Science, Engineering and Technology

(An ISO 3297: 2007 Certified Organization)

Vol. 5, Special Issue 12, May 2016

0.3	61.52	56.83	4.69
0.4	105.75	102.27	3.48
0.5	142.03	139.83	2.2
300:150:15			
0.1	101.01	100.43	0.58
0.2	76.83	74.57	2.26
0.3	72.17	67.71	4.46
0.4	106.28	102.82	3.46
0.5	118.91	115.46	3.45
300:300:15			
0.1	32.19	22.05	10.14
0.2	31.13	20.43	10.7
0.3	28.22	20.68	7.54
0.4	27.85	20.77	7.08
0.5	28.41	22.34	6.07
300:300:10			
0.1	54.59	45.34	9.25
0.2	50.70	45.86	4.84
0.3	50.00	46.88	3.12
0.4	85.60	89.15	-3.55
0.5	139.46	133.35	6.11
300:300:00			
0.1	47.21	44.20	3.01
0.2	39.19	31.56	7.63
0.3	37.29	28.43	8.86
0.4	36.11	26.02	10.09
0.5	32.33	24.05	8.28

It is evident that the E_a curve, computed using both F-W-O (Othman et al., 2015) and Kissinger methods, had a similar change trend. This explains why both methods fit into each other. However, the E_a values obtained from the F-W-O method (Othman et al., 2015) were higher than the values obtained from the Kissinger method; which were in the range 0.2 to 10.67 kJmol^{-1} . This is because β in $\ln \beta/T$ (Eq. 8) depends on the function of temperature compared to $\log \beta$ in Eq. 7.

Remarkably, possible interactions or reactions occur among Cs-Cs, MAA-MAA, MAA-MBA, Cs-MAA, Cs-MBA, etc., during degradation, or among the products of degradation; which can accelerate the degradation rate. These reactions can be grouped into the following processes, as mentioned by Titipakorn et al., (Titipakorn et al., 2007) e.g., the reaction between macromolecules and small molecules, macromolecules and small radicals, macroradicals and small molecules, two small molecules, two macroradicals or macromolecules and macroradicals. It is well-known that reactions with small molecules or small radicals can give rise to faster breakages of macromolecules and chemical structures that act as stabilizer groups. The above reasons possibly explain the occurring phenomenon and can be used to predict values on the basis of the solid state processes. Furthermore, sensitivity factors, such as the changes during the process, utilized the model-fitting methods, such as the C-Red method, which are designed to extract a single set of Arrhenius parameters for all conversion ranges.

Coats-Redfern (C-Red) method

Based on integral models, $g(\alpha)$, the C-Red equation (Eq. 9) was used to estimate the Arrhenius parameters. However, this method was unable to reveal the complexity of the process in which the obtained average value of the parameters did not reflect changes in the mechanism and kinetics with the temperature and α .

International Journal of Innovative Research in Science, Engineering and Technology

(An ISO 3297: 2007 Certified Organization)

Vol. 5, Special Issue 12, May 2016

$$\ln \frac{g(\alpha)}{T^2} = \ln \left[\frac{AR}{\beta E_a} \left(1 - \frac{2RT}{E_a} \right) \right] - \frac{E_a}{RT} \quad (9)$$

Considering Doyle's approximation that $\ln(1 - 2RT/E_a) \rightarrow 0$, (Eq. 9) is written as (Eq. 10)

$$\ln \frac{g(\alpha)}{T^2} = \ln \left(\frac{AR}{\beta E_a} \right) - \frac{E_a}{RT} \quad (10)$$

Inserting different forms of $g(\alpha)$ into (Eq. 9) results in a set of Arrhenius parameters. The linear plot of $\ln[g(\alpha)/T^2]$ versus $1/T$ makes it possible to determine E_a and $\ln(A)$ from the slope and the intercept of the graph, respectively. The E_a for all $g(\alpha)$ functions can be obtained at constant β . **Table 4** lists the E_a obtained using the C-Red method for several solid state processes at a heating rate of $20 \text{ }^\circ\text{Cmin}^{-1}$ in a nitrogen atmosphere.

Table 4.

E_a obtained using THE C-Red method for several solid state processes at β of $20 \text{ }^\circ\text{Cmin}^{-1}$ in a nitrogen atmosphere. E_a obtained by using C-Red method for several solid state processes at β of $20 \text{ }^\circ\text{Cmin}^{-1}$ in nitrogen atmosphere.

Type	E_a/RT	R^2	Type	E_a/RT	R^2	Type	E_a/RT	R^2
300:000:00			300:100:15			300:150:15		
A2	0.3728	0.6638	A2	0.1777	0.2555	A2	0.2176	0.3361
A3	0.4325	0.8399	A3	0.3984	0.7797	A3	0.4313	0.8030
A4	0.6303	0.9458	A4	0.5088	0.9038	A4	0.5381	0.9116
R1	0.0351	0.0056	R1	0.3474	0.2885	R1	0.2905	0.2187
R2	0.0875	0.0322	R2	0.4146	0.3527	R2	0.3556	0.2835
R3	0.1055	0.0453	R3	0.4376	0.3733	R3	0.3780	0.3047
D1	0.9580	0.5337	D1	1.5348	0.6761	D1	1.4397	0.6448
D2	1.0265	0.5578	D2	1.6225	0.6916	D2	1.5248	0.6617
D3	1.0989	0.5813	D3	1.7151	0.7066	D3	1.6147	0.6781
D4	1.0506	0.5659	D4	1.6533	0.6968	D4	1.5547	0.6673
F1	0.1422	0.9483	F1	0.4846	0.4130	F1	0.4236	0.3461
F2	0.6646	0.8806	F2	0.5542	0.9720	F2	0.5813	0.9730
F3	0.4413	0.8961	F3	0.2684	0.7399	F3	0.3040	0.7741
300:300:15			300:300:10			300:300:00		
A2	1.3673	0.9734	A2	1.23	0.9726	A2	1.5343	0.9984
A3	0.6641	0.9486	A3	0.5827	0.9443	A3	0.784	0.9968
A4	0.3126	0.8737	A4	0.259	0.8495	A4	0.4088	0.9925
R1	3.0608	0.9773	R1	2.7891	0.9773	R1	3.347	0.9973
R2	3.2646	0.981	R2	2.9767	0.981	R2	3.5618	0.9983
R3	3.3343	0.9821	R3	3.0409	0.9821	R3	3.6353	0.9986
D1	6.8636	0.9823	D1	6.2902	0.9825	D1	7.4107	0.9979
D2	7.1301	0.9841	D2	6.5354	0.9843	D2	7.6915	0.9985
D3	7.4108	0.9858	D3	6.7938	0.986	D3	7.9873	0.9989
D4	7.2236	0.9847	D4	6.6215	0.9849	D4	7.7901	0.9986
F1	3.4767	0.9842	F1	3.1719	0.9842	F1	3.7852	0.9991

International Journal of Innovative Research in Science, Engineering and Technology

(An ISO 3297: 2007 Certified Organization)

Vol. 5, Special Issue 12, May 2016

F2	0.1228	0.8736	F2	0.0015	0.0444	F2	0.1941	0.7107
F3	0.9877	0.9888	F3	0.8802	0.9878	F3	1.1049	0.9485

In this study, the same α values were used as those used in the F-W-O and Kissinger methods. It was found that the solid state thermal degradation mechanism of the Cs-MAA-MBA series did not fix on a single process and relied on a constituent of MAA and MBA loadings. By applying the C-Redfern approach, Cs pure was found to have better agreements with the F1 mechanism (random nucleation: Mampel first order) at $\beta=20\text{ }^{\circ}\text{Cmin}^{-1}$. These results agree with the work reported by de-Britto et al., (de Britto and Campana-Filho, 2007), which mentioned that Cs had agreements for R3 and F1 mechanisms; however, they only reported at $\beta=10\text{ }^{\circ}\text{C/min}$. It was noted that the increase in β induced thermal stress to attain a thermodynamic equilibrium, which influenced the solid state degradation mechanism.

Considering the values shown in **Table 4**, three types of solid state processes at β of $20\text{ }^{\circ}\text{Cmin}^{-1}$ in a nitrogen atmosphere were proposed as F1, F2 and F3. Each process is discussed below.

- F1; Random nucleation with one nucleus on the individual particle.
When the MAA is fixed at 300 mg/mL, the reduction content of MBA to 0mg/mL Cs hydrogel derivatives will allow the MAA to fully bind in Cs linkage to form Cs-MAA hydrogel. As a result, only one nucleus will be formed in Cs hydrogel derivatives, which are Cs-MAA. Therefore, the solid state degradation has followed the F1 process, which is random nucleation with one nucleus on the individual particle.
- F2; Random nucleation with two nuclei on the individual particle.
When the content of MBA is fixed at 15mg/mL in the Cs hydrogel derivative, the present content of MAA will initially occupy Cs-MBA linkage to form Cs-MBA-MAA. Further increasing of the MAA content will produce a Cs-MAA linkage. As a result, two miscible nuclei will be formed in Cs hydrogel derivatives, which are Cs-MBA-MAA and C nuclei s-MAA. These lead the F2 process, which is a random nucleation with two nuclei on the individual particle, and will occur below the critical point of MAA (MAA = 300mg/mL).
- F3; Random nucleation with three nuclei on the individual particle.
When the MAA content achieves the MAA limit (MAA = 300 mg/mL) in the Cs hydrogel derivative, further increasing of the MAA content will produce PMAA linkage, together with Cs-MBA-MAA and Cs-MAA. As a result, three miscible nuclei will be formed in Cs hydrogel derivatives, which are Cs-MBA-MAA, Cs-MAA and PMAA. Therefore, the solid state degradation followed the F3 process, which is random nucleation with three nuclei on the individual particle.

To adapt to this contrast, we propose that the decomposition of Cs-MAA-MBA series could be governed mainly by the molecular structure and kinetic consideration, and not by the bond energy.

IV. CONCLUSIONS

Chitosan-Methacrylic acid-N,N- methylenebisacrylamide (Cs-MAA-MBA) hydrogels at different compositions of MBA and MAA were synthesised by free radical copolymerization method in water. The non-isothermal degradation behaviour of synthesized hydrogels was studied by ThermoGravimetric Analysis (TGA) under nitrogen purge. The kinetic degradation parameters were clarified using the Kissinger method and the solid state degradation mechanism was evaluated using the Coats-Redfern (C-Red) method. The E_a obtained from the Kissinger method had a similar change trend with that of the Flynn-Wall-Ozawa (F-W-O) method; as previously reported in the article Doi:10.1016/j.indcrop.2014.12.057. However, $E_{a\text{F-W-O}} > E_{a\text{Kissinger}}$ about 0.2 to 10.67 kJmol^{-1} due to the β in $\ln \beta/T$ Kissinger method depends on the function of temperature compared to $\log \beta$ in F-W-O method. Using the C-Red method, three types of solid state processes, at β of $20\text{ }^{\circ}\text{Cmin}^{-1}$ in nitrogen atmosphere, were proposed as F1, F2 and F3, and were found to depend on an optimum composition of MAA. To adapt to this contrast, we proposed that the

International Journal of Innovative Research in Science, Engineering and Technology

(An ISO 3297: 2007 Certified Organization)

Vol. 5, Special Issue 12, May 2016

decomposition of Cs-MAA-MBA hydrogels series could be governed mainly by the molecular structure and kinetic consideration, while the solid state degradation process is dependent on the composition.

ACKNOWLEDGEMENTS

The authors wish to acknowledge the USM for sponsoring this project under USM-FRGS-6071242, USM-RU-PGRS 8046027 and the School of Materials and Mineral Resources Engineering, Engineering Campus Universiti Sains Malaysia for their technical support.

REFERENCES

1. Barral, L., Cano, J., Lopez, J., Lopez-Bueno, I., Nogueira, P., Ramirez, C., Abad, M., 1998. Thermogravimetric study of tetrafunctional/phenol novolac epoxy mixtures cured with a diamine. *J Therm Anal Calorim* 51, 489-501.
2. Coats, A., Redfern, J., 1965. Kinetic parameters from thermogravimetric data. II. *Journal of Polymer Science Part B: Polymer Letters* 3, 917-920.
3. Criado, J., Ortega, A., 1986. Non-isothermal transformation kinetics: remarks on the Kissinger method. *Journal of non-crystalline solids* 87, 302-311.
4. de Britto, D., Campana-Filho, S.P., 2007. Kinetics of the thermal degradation of chitosan. *Thermochimica Acta* 465, 73-82.
5. Dimida, S., Demitri, C., De Benedictis, V.M., Scalera, F., Gervaso, F., Sannino, A., 2015. Genipin-cross-linked chitosan-based hydrogels: Reaction kinetics and structure-related characteristics. *Journal of Applied Polymer Science*.
6. Doyle, C.D., 1965. Series approximations to the equation of thermogravimetric data. *Nature* 207, 290-291.
7. Flynn, J.H., 1997. The 'temperature integral'—its use and abuse. *Thermochimica Acta* 300, 83-92.
8. Khan, A., Othman, M.B.H., Razak, K.A., Akil, H.M., 2013. Synthesis and physicochemical investigation of chitosan-PMAA-based dual-responsive hydrogels. *Journal of Polymer Research* 20, 1-8.
9. Kissinger, H.E., 1957. Reaction kinetics in differential thermal analysis. *Analytical chemistry* 29, 1702-1706.
10. Muhd Julkapli, N., Akil, H.M., Ahmad, Z., 2011. Preparation, properties and applications of chitosan-based biocomposites/blend materials: a review. *Composite Interfaces* 18, 449-507.
11. Othman, M.B.H., Akil, H.M., Rasib, S.Z.M., Khan, A., Ahmad, Z., 2015. Thermal properties and kinetic investigation of chitosan-PMAA based dual-responsive hydrogels. *Industrial Crops and Products* 66, 178-187.
12. Ozawa, T., 1970. Kinetic analysis of derivative curves in thermal analysis. *J Therm Anal Calorim* 2, 301-324.
13. Rami, L., Malaise, S., Delmond, S., Fricain, J.C., Siadous, R., Schlaubitz, S., Laurichesse, E., Amédée, J., Montebault, A., David, L., 2014. Physicochemical modulation of chitosan-based hydrogels induces different biological responses: Interest for tissue engineering. *Journal of Biomedical Materials Research Part A* 102, 3666-3676.
14. Tiptapakorn, S., Damrongsakkul, S., Ando, S., Hemvichian, K., Rimdusit, S., 2007. Thermal degradation behaviors of polybenzoxazine and silicon-containing polyimide blends. *Polymer Degradation and Stability* 92, 1265-1278.